Laser Photonics Rev. **6**, No. 5, L1–L5 (2012) / **DOI** 10.1002/lpor.201200013

LASER & PHOTONICS REVIEWS

Abstract Optical sensing offers an attractive solution to the societal concern for prevention of natural and human-generated threats and for efficient use of natural resources. The unprecedented properties of optical fibers make them ideal for implementing a 'nervous system' in structural health monitoring: they are small, low-cost and electrically and chemically inert. In particular, the nonlinear interaction of stimulated Brillouin scattering allows for the distributed measurement of strain and temperature with tens of km range. In this work, a novel, radar-inspired technique for random-access Brillouin scattering-based sensors is shown, making a significant step towards a real optical sensing nerve. The method selectively addresses each fiber segment as a distinct sensing element in a synaptic neuronal system. The measurement principle relies on phase-coding of both the Brillouin pump and signal waves by a high-rate, pseudo-random bit sequence. Temperature measurements with 1 cm resolution are reported. The measurement range is scalable to several km.

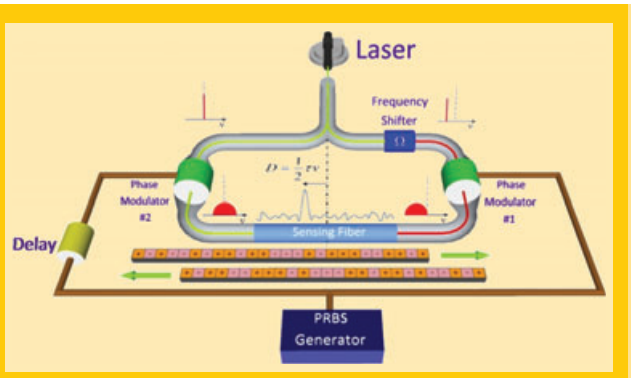

LETTER ARTICLE

Random-access distributed fiber sensing

Avi Zadok[1,*], Yair Antman[1], Nikolay Primerov[2], Andrey Denisov[2], Juan Sancho[2,3], and Luc Thévenaz[2]

The precision localization of disturbances has been a mainstay of radar systems since WW-II. A widely employed radar technique relies on the transmission of long sequences of short pulses [1], and their subsequent processing by a pre-designed matched filter at the receiving end. The filtering procedure compresses the sequence of pulses to a temporally-narrow impulse response function, which provides high resolution together with a large signal to noise ratio [1]. Matched filters in radars are realized by correlating the received radar echoes against a replica of the transmitted sequence, which was stored as a reference. The correlation, in turn, is implemented either through ratio-frequency, electrical analogue mixing or via digital signal processing. Correlation coding has been introduced to Rayleigh scattering-based optical time-domain reflectometry, as early as 1989 [2]. In our work, we carry over the principle of match-filtering long pulse sequences to the realm of fiber-optic sensing [3–7], and use it for the unambiguous probing of a random locale. Stimulated Brillouin scattering (SBS) is an ideally suited platform for such random-access sensing system: not only is it inherently dependent on both strain and temperature [8–12], it also allows for the realization of correlation-based matched filtering of pulse sequences *directly in the optical domain*, as will be described in detail.

In stimulated Brillouin scattering (SBS), a relatively intense pump wave interacts with a counter-propagating signal wave, which is detuned in frequency [8]. The combination of the two waves generates an intensity beating pattern, whose frequency equals the difference Ω between the two optical frequencies. Through electrostriction, the intensity beat introduces an acoustic wave, which in turn leads to a traveling grating of refractive index variations, due to the photo-elastic effect. The traveling grating can couple optical power between the pump and signal waves. Effective coupling, however, requires that Ω should closely match a fiber-dependent parameter known as the *Brillouin frequency shift* $\Omega_B \sim 2\pi \cdot 11$ GHz [8]. The bandwidth of SBS driven by a continuous pump wave is only 30 MHz, as decreed by the relatively long phonon lifetime $\tau \sim 5$ ns [8]. The value of Ω_B varies with both temperature and strain [9–12], hence an assessment of the *local* Ω_B may provide a distributed measurement of either of these two parameters [9–12].

SBS-based distributed measurements are commercialized for over 15 years. Most available systems rely on Brillouin optical time domain analysis (B-OTDA) techniques, in which the pump and / or signal waves are pulsed [13]. The power gain of the signal is observed as a function of both Ω and the time of arrival, signifying position. The spatial resolution of B-OTDA is fundamentally restricted to about 1 meter [14]: the use of pulses shorter than τ both reduces the SBS interaction length and broadens its linewidth [14]. Numerous techniques have been proposed in recent years for the enhancement of B-OTDA resolution [15, 16], such as the pre-excitation of the acoustic wave [17, 18], dark [19] and π-phase [20, 21] pump pulses, repeated measurements with pump pulses of different widths [22], differentiation of the probe power [23] and many more. Such methods considerably increase the complexity of the B-OTDA instrument. The range and signal-to-noise ratios of long-reach B-OTDAs have been improved considerably by encoding

[1] Faculty of Engineering, Bar-Ilan University, Ramat-Gan 52900, Israel
[2] Ecole Polytechnique Fédérale de Lausanne, Institute of Electrical Engineering, SCI-STI-LT Station 11, 1015 Lausanne, Switzerland
[3] Permanent address: iTEAM Institute, Universidad Politécnica de Valencia, 46022 Valencia, Spain
[*] Corresponding author: e-mail: Avinoam.Zadok@biu.ac.il

pulse sequences [24–27], however these methods did not address high resolution measurements.

An alternative solution path is that of Brillouin optical correlation-domain analysis (B-OCDA). Rather than rely on pulses, it is based on the synchronous frequency modulation of constant-magnitude pump and signal waves, nominally detuned by Ω, by a common sine wave [28, 29]. The instantaneous difference in frequency between the two counter-propagating waves remains fixed at particular fiber locations only, known as correlation peaks, whereas the frequency difference elsewhere is oscillating [28]. Consequently, effective SBS amplification is confined to the narrow correlation peaks. However, the unambiguous measurement range is restricted to the separation between periodic correlation peaks. When simple sine-wave frequency modulation is used, the measurement range is on the order of a few hundred resolution points. The method had recently been extended to multiple modulation frequencies, resulting in 27 cm resolution over 1.5 km range [30]. B-OCDA also allows for dynamic strain analysis, monitoring vibrations of frequencies as high as 200 Hz [31].

In this work, we propose and demonstrate a new paradigm for SBS-based distributed sensing, which significantly extends its state of the art in terms of range versus resolution trade-off. The random-access sensing principle is illustrated in Fig. 1. Similarly to matched-filtering processing in radars, both Brillouin pump and signal waves are jointly phase-modulated by a common binary pseudo random bit sequence (PRBS), whose symbol duration T is much shorter than τ [32]. The modulation phase within each symbol assumes a value of either 0 or π, with equal probabilities. Suppose at first that the phase modulation is synchronized so that the two waves are of equal phases at their respective entry points. The instantaneous driving force for the SBS acoustic field generation is proportional to the product of the pump wave envelope and the complex conjugate of the signal wave envelope [8]. We may therefore distinguish between the dynamics of the SBS-induced acoustic field in two different regions. In the vicinity of the fiber center the pump and signal are correlated, hence their phase difference is constant and the driving force for the acoustic field generation keeps a steady non-zero value. Consequently, the acoustic field is allowed to build up to its steady state value, and permits the interrogation of the local Brillouin shift. The width of the correlation peak is on the order of $\Delta z = \frac{1}{2} v_g T$, where v_g is the group velocity of light in the fiber [32]. In all other locations, the driving force for the acoustic field is randomly alternating in sign on every symbol duration $T \ll \tau$. The acoustic field magnitude thus averages out to a zero expectation value, and the SBS interaction outside the correlation peak is largely inhibited [32]. The profile of the acoustic field that is generated in the fiber is equivalent to the impulse response function of a match-filtered, spread-time radar sequence ([1], see Fig. 1). The phase modulation broadens the power spectral density of the pump wave, and elevates the threshold of depletion due to spontaneous Brillouin scattering.

The SBS interaction subject to the above modulation scheme is both localized and stationary, so that measurement noise can be averaged out over detection intervals of choice. The separation between adjacent correlation peaks equals $\frac{1}{2} M v_g T$, where M is the PRBS length. The unambiguous measurement range can be made arbitrarily long, while retaining the above high resolution Δz [32]: PRBS generators readily provide sequences that are 2^{31}-1 bits long, corresponding to more than 2 billion resolved points. Compared with current B-OCDA techniques, PRBS coding provides a simpler route towards longer measurement ranges, thereby constituting a sensing platform that is truly random-access in nature. The principle described above is addressed in more mathematical detail in supplementary information item 1. A conceptual sketch of a random-access sensing system based on the above principle is depicted in Figure 2.

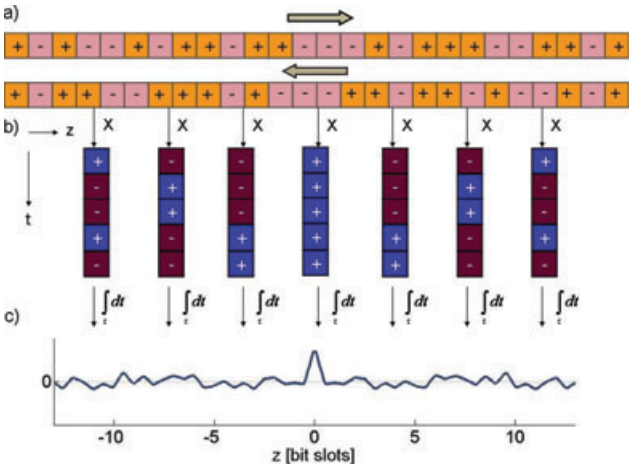

Figure 1 (online color at: www.lpr-journal.org) The principle of random access distributed fiberoptic sensing using SBS. a) Illustration of binary phase modulated Brillouin probe wave complex envelope, propagating in the positive z direction (top row). The sign of the optical field randomly alternates in between symbols through binary phase modulation. Bottom row: the SBS pump wave complex envelope, comodulated by the same binary phase sequence, and propagating in the opposite direction. b) The instantaneous driving force for the generation of the SBS acoustic field is proportional to the inner product between the pump envelop, and the complex conjugate of the signal envelope. Therefore, a constant driving force prevails at discrete peak locations only (center), in which the two replicas of the modulation sequence are in correlation. Elsewhere, the driving force is oscillating. c) The magnitude of the resulting acoustic field, obtained by temporal integration over the driving force (see supplementary information item 1 for more detail). The Brillouin interaction performs a match filtering operation directly in the optical layer.

A detailed drawing of the specific setup used in our experiments is illustrated in Fig. 3. Light from a distributed feedback (DFB) laser diode of frequency ω_0 was used as the source of both pump and signal. The DFB output passed through an electro-optic phase modulator, driven by a PRBS generator. The generator clock rate $1/T$ was in the range of 8–12 GHz, corresponding to Δz between 0.9 cm and 1.3 cm, and the code length was $M = 2^{15} - 1$. The modulator driving voltage was adjusted to match its V_π. The modulated wave

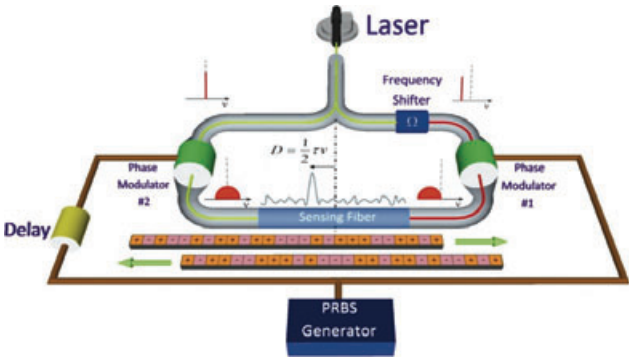

Figure 2 (online color at: www.lpr-journal.org) A schematic illustration of a setup for arbitrary access, high resolution Brillouin optical time domain analysis. Both pump and signal waves are drawn from the output of a single monochromatic laser. The signal wave is offset in frequency by Ω, which is on the order of the Brillouin frequency shift in the fiber under test. Both waves are comodulated by a common PRBS phase code, and launched from opposite ends of the fiber under test. Careful timing of the two phase modulators provides a scan of the code correlation peak across the fiber, and allows for the arbitrary addressing of specific points. The Brillouin gain spectrum in each point is reconstructed through varying Ω.

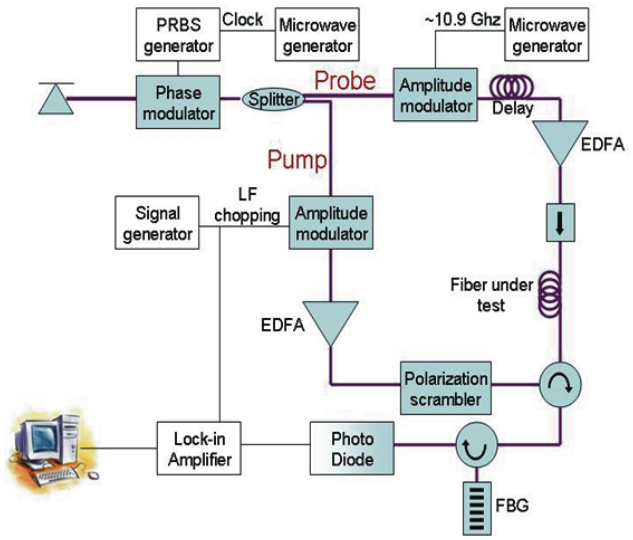

Figure 3 (online color at: www.lpr-journal.org) Experimental setup for random access SBS based distributed sensing. LF: low frequency. FBG: fiber Bragg grating. EDFA: erbium doped fiber amplifier. A path length imbalance was introduced in the probe branch, so that the fiber under test was in overlap with an offcentered correlation peak. The position of the correlation peak could be varied through changing the symbol duration T.

was split into pump and signal paths. In the signal branch, an amplitude electro-optic modulator was used to generate two modulation sidebands at frequencies $\omega_0 \pm \Omega$, the lower of which was subject to SBS amplification. The modulator was biased to suppress the carrier wave at ω_0. The signal wave was amplified and launched into one end of a fiber under test. Light in the pump branch was amplitude-modulated by a low-frequency sine wave, amplified to 500 mW, and launched into the opposite end of the fiber under test. A polarization scrambler was used in the pump arm, in order to avoid potential polarization-related fading [33]. Note that a single phase modulator is used in the coding of both pump and probe optical waves.

Arbitrary locations along the fiber under test were addressed as follows. The joint phase modulation introduces multiple correlation peaks along the fiber ring that encompasses the pump branch, the probe branch, and fiber under test. The peaks are separated by $\frac{1}{2}Mv_gT$, hence the position of all peaks, except for the central one, vary with T. A path imbalance was inserted along the signal branch, so that an off-centered correlation peak was in overlap with the fiber under test. The position of this peak could be scanned through slight changes to the PRBS symbol duration: 1 MHz variation of the clock rate corresponded to an offset of the correlation peak by 34 cm. At the same time, the code length was sufficiently long to guarantee that only one peak occurs within the fiber under test.

The output signal was filtered by a fiber-Bragg grating which retained only the sideband of interest at $\omega_0 - \Omega$, and detected by a photo-diode. The detected current was analyzed by the lock-in-amplifier, tuned to the low modulation frequency of the pump wave. Hence potential contribution from spontaneous Brillouin scattering at the signal wave frequency was suppressed. The Brillouin gain spectrum in each fiber locale was reconstructed through measuring the power of the amplified output signal wave as a function of Ω.

Figure 4 shows measurements along a sensing single mode fiber, which consisted of several non-identical seg-

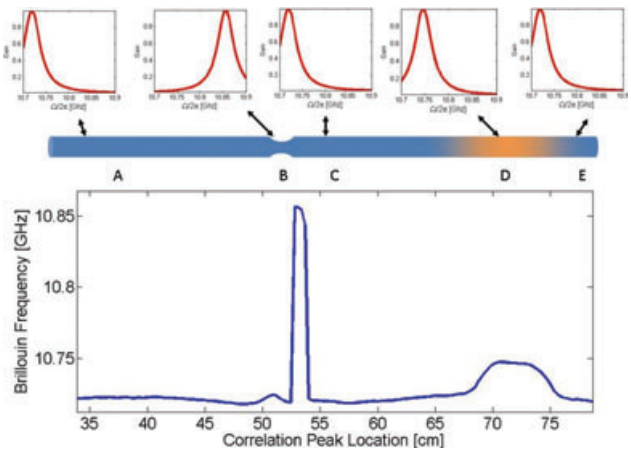

Figure 4 (online color at: www.lpr-journal.org) Brillouin gain mapping of a fiber under test, comprised of a 1 cm-long section of spliced dissimilar fiber (point B), and a 7 cm-long heated section (point D). The Brillouin gain spectra of different points along the fiber are resolved using the random access sensing methods (see insets for addressing points A through E). The Brillouin frequency shifts for points B and D are different from the background values (points A, C, E). The lower curve shows the extracted Brillouin frequency shift after addressing sequentially all positions. Note the sharp edges of the dissimilar spliced fiber, as opposed to the gradual profile of the heated section (heat conduction).

ments spliced together. One section was 1 cm-short. In addition, a 7 cm-long section of the fiber was locally heated by a resistor. Deviations in the Brillouin gain spectrum are evident in all heated and spliced sections. Figure 5 shows measurements of an entire 40 m-long fiber, in which a 1 cm-long heated section is resolved. Lastly, the figure also demonstrates the random-access monitoring of 9 mm-long sections at arbitrary locations along 200 meters of fiber under test, and the localization of a 1 cm-long hot spot along the same fiber. The continuous scanning of the entire 200 meters-long fiber with over 20,000 resolution points, using the equipment available to us, required a prohibitively long duration. The limitation can be readily overcome using state-of-the-art electronics, and it is not fundamental.

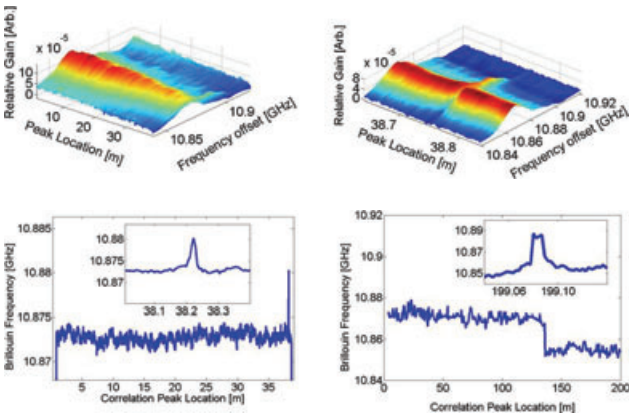

Figure 5 (online color at: www.lpr-journal.org) Top left – Brillouin gain mapping of a 40-meter-long fiber with 1 cm resolution, corresponding to 4000 resolved points. A 1 cm-long section of the fiber was locally heated. Top right – magnified view of the Brillouin gain map in the vicinity of the heated section. Bottom left – corresponding measured Brillouin frequency shift as a function of position. The region immediately surrounding the heated section is magnified in the inset. The standard deviation on this estimation along a uniform fiber section is 0.5 MHz, corresponding to a temperature inaccuracy of ± 0.5 °C. Bottom right – Brillouin frequency shift measurements over a 200-meters-long fiber, with sub cm resolution. 330 arbitrarily located sections of the fiber under test are randomly addressed. The interrogated sections are only 9 mm long, evenly spaced by approximately 60 cm. The fiber under test consisted of two dissimilar segments spliced together. The inset shows measurements of the Brillouin shift in the vicinity of a 1 cm-long hot spot, located at the end of the fiber. (The 330 randomly addressed sections of the main panel did not coincide with the hot spot).

The results illustrate the random-access point interrogation of the fiber under test, since each centimeter-long segment of the fiber can be addressed separately and selectively. The measurement range would be restricted eventually by its signal-to-noise ratio. The signal amplification over a cm-long correlation peak is weak, while fluctuations due to residual off-peak scattering scale with the length of the fiber under test [32]. These fluctuations are averaged out over measurement durations that are orders-of-magnitude longer than the symbol duration [32]. Altogether, our calculations suggest that the measurement signal to noise would limit its range to the order of 1 km for 1 cm resolution, or 100,000 resolution points.

Finally, the localization method is equally applicable to the generation of dynamic acoustic gratings over polarization maintaining fibers [32, 34–36]. Such gratings allow for the distributed measurement of both Ω_B and local birefringence [35, 36]; provide variable optical delays that are free of the delay-bandwidth product limitations [32]; and may serve in all-optical correlators of electrical data and in tunable microwave photonic filters [37].

Acknowledgements. This work was supported by the Swiss National Science Foundation through project 200021-134546, by the European Community's Seventh Framework Programme [FP7/2007-2013] under grant agreement no. 219299 (GOSPEL project), by the Israeli Science Foundation (ISF), by the KAMIN program of the Chief Scientist Office of the Israeli Ministry of Industry, Trade and Labor, and was realized in the collaborative framework of the COST Action TD1001 OFSESA.

Received: 21 March 2012, **Revised:** 23 May 2012, **Accepted:** 8 June 2012

Published online: 28 June 2012

Key words: Fiber-optic sensing, stimulated Brillouin scattering, all-optical signal processing, distributed measurements.

Supporting information for this article is available free of charge under http://dx.doi.org/10.1002/lpor.201200013.

References

[1] N. Levanon and E. Mosezon, Radar Signals (John Wiley & Sons, Hoboken, NJ, 2004).
[2] M. Nazarathy, S. A. Newton, R. P. Giffard, D. S. Moberly, F. Sischka, W. R. Trutna, and S. Foster, L. Lightwave Technol. **7**, 24–38 (1989).
[3] B. Culshaw and J. Dakin, Optical Fiber Sensors: Principles and Components (Artech House, Boston, MA, 1988).
[4] K. T. V. Grattan and B. T. Meggit (eds.), Optical Fiber Sensor Technology (Kluwer academic publishers, Dordrecht, 2000).
[5] K. T. V. Grattan and B. T. Meggit (eds.), Optical Fiber Sensor Technology Volume 4, Chemical and Environmental Sensing (Kluwer academic publishers, Dordrecht, 2010).
[6] E. Udd and W. B. Spillman WB (eds.), Fiber Optic Sensors: An Introduction for Engineers and Scientists, Second Edition (John Wiley & Sons, Hoboken, NJ, 2011).
[7] E. Udd (ed.), Fiber Optic Smart Structures (John Wiley & Sons, New York, NY, 2011).
[8] R. W. Boyd, Nonlinear Optics, third edition (Academic Press, Burlington, MA, 2008).
[9] T. Kurashima, T. Horiguchi, and M. Tateda, Opt. Lett. **15**, 1038–1040 (1990).
[10] T. Horiguchi, T. Kurashima, and M. Tateda, IEEE Photonic. Tech. L. **2**, 352–354 (1990).
[11] X. Bao, D. J. Webb, and D. A. Jackson, Opt. Lett. **18**, 552–554 (1993).
[12] M. Niklès, L. Thévenaz, and P. A. Robert, Opt. Lett. **21**, 758–760 (1996).
[13] T. Horiguchi and M. Tateda, Opt. Lett. **14**, 408–410 (1989).

[14] A. Fellay, L. Thevenaz, M. Facchini, M. Nikles, and P. A. Robert, in: Proceedings of the Optical Fiber Sensors Conference (OFS-12), 324–327 (1997).
[15] J. C. Beugnot, M. Tur, S. Foaleng Mafang, and L. Thévenaz, Opt. Express **19**, 7381–7397 (2011).
[16] X. Bao and L. A. Chen, Sensors **11**, 4152–4187 (2011).
[17] V. Lecoeuche, D. J. Webb, C. N. Pannell, and D. A. Jackson, Opt. Lett. **25**, 156–158 (2000).
[18] F. Wang, X. Bao, L. Chen, Y. Li, J. Snoddy, and X. Zhang, Opt. Lett. **33**, 2707–2709 (2008).
[19] A. W. Brown, B. G. Colpitts, and K. Brown, IEEE Photonic. Tech. L. **17**, 1501–1503 (2005).
[20] L. Thévenaz and S. Foaleng Mafang, in: Proceedings of 19th International Conference of Fiber Sensors, SPIE, Perth, WA, Australia, Proc. SPIE **7004**, 70043N, 70043N-4 (2008).
[21] S. Foaleng Mafang, M. Tur, J. C. Beugnot, and L. Thevenaz, J. Lightwave Technol. **28**, 2993–3003 (2010).
[22] W. Li, X. Bao, Y. Li, and L. Chen, Opt. Express **16**, 21616–21625 (2008).
[23] T. Sperber, A. Eyal, M. Tur, and L. Thevenaz, Opt. Express **18**, 8671–8679 (2010).
[24] M. A. Soto, G. Bolognini, F. D. Pasquale, and L. Thevenaz, Opt. Lett. **35**, 259–261 (2010).
[25] M. A. Soto, G. Bolognini, F. D. Pasquale, and L. Thevenaz, Meas. Sci. Technol. **21**, 094024 (2010).
[26] X.-H. Jia, Y.-J. Rao, L. Chang, C. Zhang, and Z.-L. Ran, J. Lightwave Technol. **28**, 1624–1630 (2010).
[27] X.-H. Jia, Y.-J. Rao, K. Deng, Z.-X. Yang, L. Chang, C. Zhang, and Z.-L. Ran, IEEE Photonics Tech. L. **23**, 435–437 (2011).
[28] K. Hotate and T. Hasegawa, IEICE T. Electron. **E83-C**, 405–412 (2000).
[29] K. Hotate and M. Tanaka, IEEE Photonics Tech. L. **14**, 179–181 (2002).
[30] Y. Mizuno, Z. Y. He, and K. Hotate, Opt. Express **18**, 5926–5933 (2010).
[31] K. Y. Song and K. Hotate, Proceedings of SPIE **6770**, 67700J (2007).
[32] Y. Antman, N. Primerov, J. Sancho, L. Thevenaz, and A. Zadok, Opt. Express **20**, 7807–7821 (2012).
[33] A. Zadok, E. Zilka, A. Eyal, L. Thevenaz, and M. Tur, Opt. Express **16**, 21692–21707 (2008).
[34] K. Y. Song, W. Zou, Z. He, and K. Hotate, Opt. Lett. **33**, 926–928 (2008).
[35] Y. Dong, X. Bao, and L. Chen, Opt. Lett. **34**, 2590–2592 (2009).
[36] K. Y. Song, S. Chin, N. Primerov, and L. Thevenaz, J. Lightwave Technol. **28**, 2062–2067 (2010).
[37] J. Sancho, N. Primerov, S. Chin, Y. Antman, A. Zadok, S. Sales, and L. Thévenaz, Opt. Express **20**, 6157–6162 (2012).